

# A visualization study of a flow-induced acoustic resonance in closed side branches

76899 李 艷榮  
指導教員 染矢 聡 准教授

In this study, flow-induced acoustic resonance in a piping system containing tandem closed side-branches was investigated experimentally. An instantaneous velocity field in a cross section was visualized two-dimensionally using high-time-resolved PIV, simultaneously with the pressure measurement at multi-points around the cavity by microphones. Consequently, phase delays of oscillation at different points were obtained two-dimensionally. 2-D phase map was helpful to discuss the feedback mechanism of the self-induced vibration. The interactions between the oscillating flows in different cavities were also discussed in the present research. An uncommon acoustic mode change was observed when the flow rate in the main pipe increased.

Key words: Visualization, Flow-induced acoustic resonance, closed tandem side branches, PIV

## 1 Introduction

Systems with closed side-branch pipes are liable to an excitation of sound with discrete frequency components. When high velocity steam/gas passes safety relief valves, it may produce acoustic resonance in the valves and subsequent noise, excessive vibration. Flow and acoustic phenomena associated with closed single, co-axial or tandem branches have been studied for many years. The outbreak mechanism of cavity tone has been ascertained by phase-averaged pressure measurements in previous researches. A few visualization studies were done but there was no other research using PIV technique. In the present study, flow-induced acoustic resonance in a piping system containing closed co-axial and tandem side-branches was investigated experimentally. In this report, the mechanism of tandem branches was discussed in detail. The frequency of sound vibration was more than a few hundred Hz. The visualization method used in present experiments is the high-time-resolved Particle Image Velocimetry (PIV) technique. The phase delay map in the visualization area was obtained from the analyzed velocity at the dominant frequency. This is the first two-dimensional experimental investigation to detect the time sequential instantaneous velocity field with long side branches ( $L/D \gg 1$ ) and high inflow velocity at high resonant frequency.

## 2 Experimental setup and methods

The experimental setup was designed to actualize direct observation of the flow in the cross section of the side branches, and was shown schematically in Fig. 1.

The flow-generating unit consists of two pumps. The flow rate of each pump was controlled by a sonic nozzle. The mass flow meters were installed at the delivery end of each pump. The air coming from pump 1 flowed through an oil mist generator with Laskin nozzle. The air was seeded with oil mist particles (olive oil with a mean diameter of  $3\mu\text{m}$ ). Because the Stokes number was much smaller than 1, the particles could follow the fluid flow closely. Pump 2 was used to control the total

mass flow rate and the number density of the particles in the working fluid. The total flow rate  $Q$  ranged from 30 l/min to 39 l/min. In previous experiments, many researchers supplied a large mass flow in the main pipe to obtain a high mean velocity and a high shear flow velocity. Ziada & Bühlmann<sup>1)</sup> have provided maximum flow rate of  $2000 \text{ m}^3 / \text{hr}$  and maximum Reynolds number of  $0.26 \times 10^6$  to the onset of resonance. In the present study, the experiments were done with high local mean velocity at the mouth of the cavity with the small mass flow-rate. A generation of the self-induced vibration with large amplitude needs high local mean velocity at the mouth of the cavity. To supply high speed shear flow is more important than giving large total mass flow in the main pipe. Therefore, a block was put at the upstream side of the cavity to form high local mean velocity at the mouth of the cavity in our system. The two pipes forming the tandem geometries were of equal length.

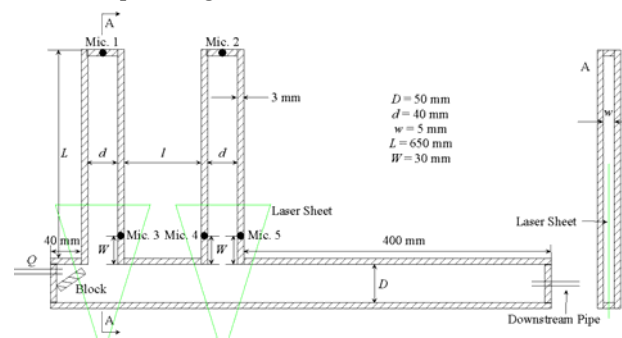


Fig. 1 Schematic of the experimental setup

Five SiSonic microphones (SP0103NC3-3, Dover Co. Ltd.) with integrated amplifier were put at the closed side branches to detect the acoustical pressure, the positions of the microphones were shown in Fig. 1.

The two-dimensional velocity fields were measured using the PIV technique. A high frequency double pulsed laser ( $\lambda = 527 \text{ nm}$ ) was chosen to produce a thin light sheet to illuminate the test section (1 mm in thickness and with a probing area of  $45 \times 45 \text{ mm}^2$ ).

A high-speed camera captured an image of the particles in the flow field at each pulse, at a speed of

6000 frames per second (fps) with a resolution of 1024 x 1024 pixels. 2729 image pairs were processed and analyzed using the recursive cross-correlation PIV. For PIV cross correlation, the initial interrogation window size was 64 x 64 pixels and the last interrogation size was 32 x 32 pixels. The search window size was set equal to 20 and 10 pixels.

### 3 Results and Discussions

It has been demonstrated in the literature<sup>1)</sup>, that for piping systems with long side-branches ( $L/D \gg 1$ ) and large diameter ratio ( $d/D \approx 1.0$ ), the resonance frequency of tandem side-branches at each mode at atmospheric pressure can be accurately predicted by eq.(1) based on the length of the side-branches,  $L$ , the speed of sound,  $C$ , and the distance between two branches,  $l$ , where  $m$  is

$$f_m = \frac{C(2m-1)}{4(L+l/2)}, m = 1, 2, 3... \quad (1)$$

the acoustic mode number. All experiments were performed at the room temperature of 23°C in the laboratory,  $C = 345.3$  m/s in this condition. From eq.(1), the frequencies of the acoustic modes in our system are estimated at 123.3 Hz and 369.9 Hz when  $m = 1$  and 2. Here after, the oscillation mode for  $m = 1$  is called first mode and that for  $m = 2$  is called third mode.

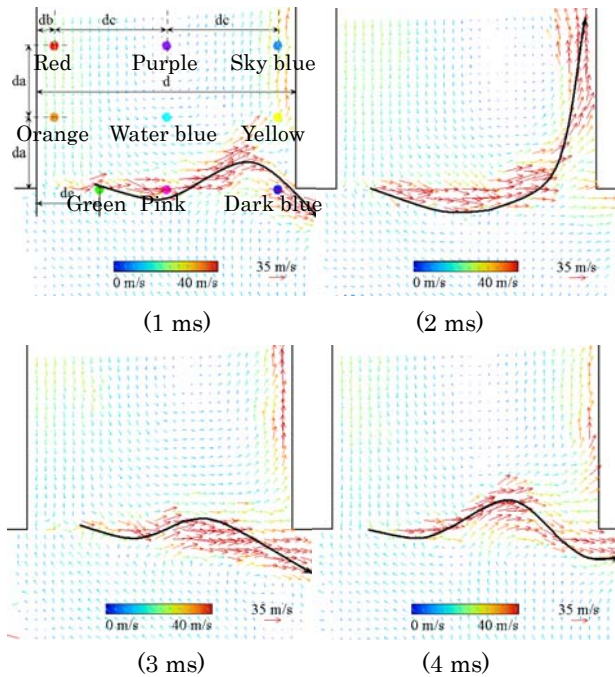


Fig. 2 Measured velocity vector maps for  $Q = (5.5 + 28)$  l/min in the first branch

#### 3.1 Results for $Q = (5.5 + 28)$ l/min in the first branch

Fig. 2 shows the calculated velocity fields in the visualization area. The vector in the lower right corner indicates a magnitude of 35 m/s. One can clearly see the fluctuation of the shear layer from these time sequential instantaneous velocity fields. Parameters in Fig. 2 (1ms):  $da$ ,  $db$ ,  $dc$  and  $de$  show the level of different

points in the visualization area which have a range of  $da = 0.276d$ ,  $db = 0.069d$ ,  $dc = 0.431d$  and  $de = 0.241d$ , respectively. It can be deduced from this figure that: the shear-layer perturbations are amplified and convected downstream. When the flow impinged on the trailing edge, one part flowed into the branch and the other part flowed through the main pipe. The fluids into the branch interact with the acoustic field and form a large vortex to feedback the velocity fluctuation into the upstream side of the cavity. This fluctuation induces new perturbations in the unstable shear layer at the separation point. These processes are consistent with the general “fluid-resonant mechanism<sup>2)</sup>” and “feedback mechanism” of the edge-tone.

The dominant frequency of the velocity fluctuation by FFT-analysis ( $f_{PIV}$ ) at different points in the cavity and the acoustic frequency by microphones ( $f_{MIC}$ ) were all about 345.7 Hz. The local mean velocity at the mouth of the cavity was 36.2 m/s, so that the jet fluctuation frequency was 906 Hz and the Strouhal number was 0.38. In the present flow condition,  $m$  was equal to 2, and the frequency estimated from eq.(1) was 369.9 Hz, which was consistent with  $f_{PIV}$  and  $f_{MIC}$ . The difference between them is -7.0%.

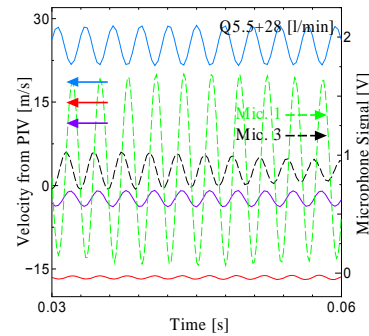


Fig. 3 Band-passed microphone signals of Mic. 1, Mic. 3 and vertical component of the detected velocity vectors

Band-passed microphone signals and band-passed vertical component of the detected velocity vectors are shown in Fig. 3. The different colors of the curve in this figure are corresponding to the points in the cavity of the measured velocity vector map (Fig. 2 (1ms)). The average value of the velocity fluctuation at the red, purple and sky blue points are -16.56 m/s, -2.39 m/s and 25.24 m/s, respectively, and that for Mic. 1 and Mic. 3 are 0.877 V and 0.869 V. After using the band pass filter to cut off the high & low frequency component ( $>356$  Hz &  $< 336$  Hz), the phase difference between different points was shown clearly. According to this kind of figure, the phase difference between the green and pink points in Fig. 2 (1ms) is  $-54^\circ$ , between the pink and dark blue points,  $-167^\circ$ , between the orange and water blue points,  $-12^\circ$ , between the water blue and yellow points,  $-179^\circ$ , between the red and purple points,  $-17^\circ$ , and that between the purple and sky blue is  $-173^\circ$ .

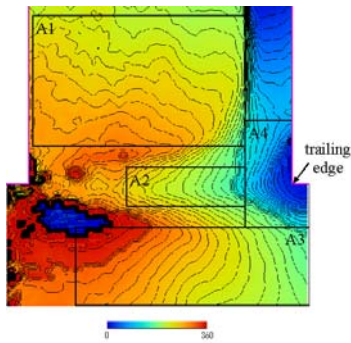


Fig. 4 Contour map of phase difference in the first branch for  $Q = (5.5 + 28)$  l/min

The contour map of phase difference in the first branch at the frequency of 347 Hz is shown in Fig. 4. The contour interval is  $10^\circ$ . This figure was obtained from calculating the cross-correlation value for the vertical component of the relative velocity fluctuations at different points. This is the first research which can obtain this kind contour map using the time sequential instantaneous velocity fields. From this figure, one can obtain the phase difference between any two points. The phase delay between two points which keeps a certain distance at A1, A2 and A3 is much smaller than that at A4. The phase delay at the trailing edge becomes large dramatically. This indicates that the difference of oscillating velocity component at the cavity-tone frequency between two points at a certain interval is larger in this area. So the energy supply for the oscillation in this area is larger than that in other areas. The propagation of the velocity perturbation in the shear flow becomes faster when the shear flow convected downstream. This suggests that the oscillating jet is affected by the structure of the trailing edge. Furthermore, this implies that the shear flow near the trailing edge was deflected by the trailing edge and momentum was delivered into the branch. The phase difference contour line around the jet flow is nearly symmetry. However, the farther the points away from the shear flow, the more asymmetric the contour line becomes. The contour line in the cavity and in the main pipe is totally different, due to the existence of the side branch.

### 3.2 Results for $Q = (5.5+28)$ l/min in the second branch

The measured velocity vector maps for  $Q = (5.5 + 28)$  l/min in the second branch are presented in Fig. 5. The vector at the center top indicates a magnitude of 3.5 m/s. The upstream flow in the main pipe was rightward, but the flow direction changed into leftward at the mouth of the second branch. By checking all the instantaneous velocity vector maps at this flow rate, it was found that the velocity vectors near the upstream side wall of the branch were always upward, as shown in Fig. 5 (a). Dominant frequency of the velocity fluctuation by FFT-analysis ( $f_{PIV}$ ) at different points in this branch and the acoustic frequency simultaneously

detected by microphones ( $f_{MIC}$ ) were all about 347.2 Hz, not so different from 345.7 Hz, which obtained in the first branch. The difference is caused by the existence of the flow, which is not considered in eq.(1).

The experimental evidence of the study performed by Jungowski et al.<sup>3)</sup> shows that the resonance in the system as a whole, not in the branch alone, determines the tone amplitude, which varies considerably with the acoustic field in the main pipe. The phase difference between any two points in the second branch was small, not far from  $0^\circ$ . There was no phase propagation in the shear flow, as shown in Fig. 5 (b). In addition, the phase difference between pressure fluctuations at Mic.1 and at Mic.2 was nearly equal to  $180^\circ$ . Thus, the second branch seems to be just a resonator.

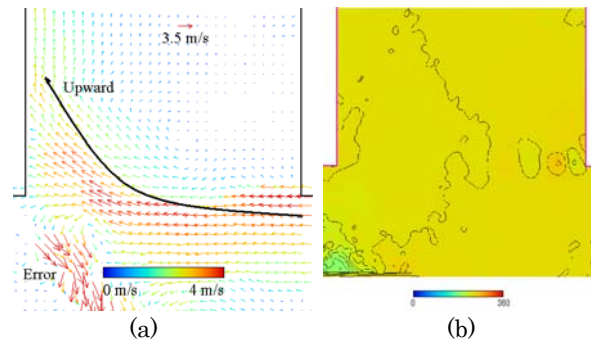


Fig. 5 Measured velocity vector map (a) and contour map of phase difference (b) for  $Q = (5.5 + 28)$  l/min in the second branch

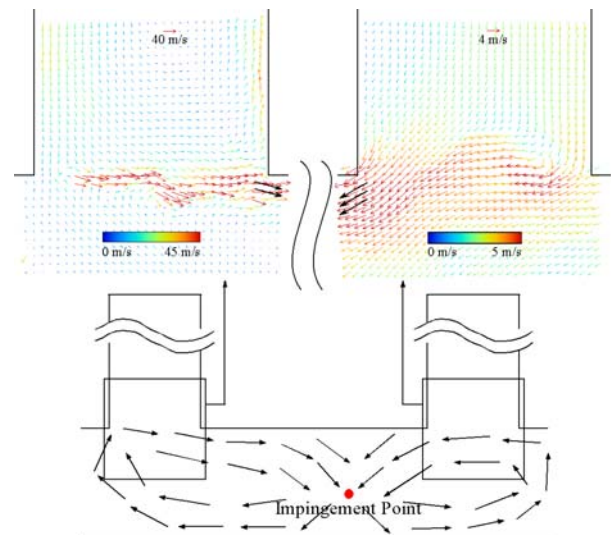


Fig. 6 Measured velocity vector maps for  $Q = (5.5 + 31)$  l/min in two branches (upper) and schematic flow pattern in the main pipe (lower)

### 3.3 Results for $Q = (5.5 + 31)$ l/min in both branches

The PIV result of the time-averaged velocity vector maps in the two branches for  $Q = (5.5 + 31)$  l/min were not so different from those for  $Q = (5.5+28)$  l/min. However, the instantaneous velocity vector maps were quite different between two cases. The velocity vectors at inside of the second cavity were all downwards at

the moment shown in Fig. 6, but there were no such moment when  $Q = (5.5 + 28)$  l/min. The lower figure in Fig. 6 shows the schematic flow direction in the main pipe. Dominant frequency of the velocity fluctuation by FFT-analysis ( $f_{PIV}$ ) at different points in both branches and the acoustic frequency by microphones ( $f_{MIC}$ ) for  $Q = (5.5+31)$  l/min were all about 115.7 Hz, as shown in Fig. 7. It seems the acoustic mode  $m$  is equal to 1 in this case. When  $m=1$ , the frequency estimated from eq.(1) is 123.3 Hz, which is consistent with  $f_{PIV}$  and  $f_{MIC}$ . The difference between them is -6.6%. From Fig. 7, one can observe that the dominant frequency change to a smaller value when the flow rate is increased. In previous studies, the oscillating mode always shifts from the lower mode to the higher mode, when the flow rate in the main pipe is increased. This is the first research that one can see the acoustic mode change from higher mode to lower mode, from both the microphone results and the PIV results.

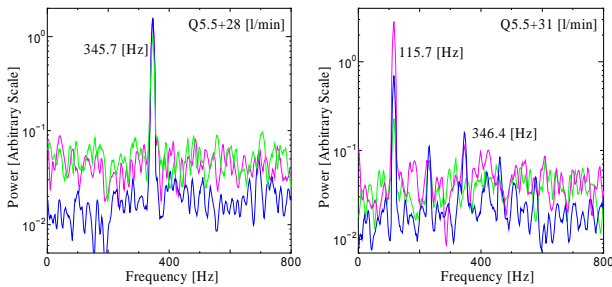


Fig. 7 Dominant frequency of the velocity fluctuation by FFT-analysis at different points in the first branch for different flow rate

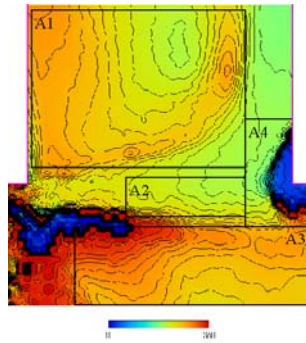


Fig. 8 Contour map of phase difference in the first branch for  $Q = (5.5 + 31)$  l/min

The contour map of phase difference in the first branch for  $Q = (5.5 + 31)$  l/min at the frequency of 116 Hz is shown in Fig. 8. The contour interval and method to obtain this figure are the same as for Fig. 4. Compare with Fig. 4, one can see the contour line is totally different at A1, A2 and A3. These differences show the effect of the flow from the second branch on the flow in the first branch. The propagation of the velocity perturbation in the shear flow (A2) is smaller than that at A3, although that in the shear flow (A2) is bigger than that at A3 for  $Q = (5.5+28)$  l/min. This suggests that the high propagation velocity at A3 is

caused by the flow from the second branch not by the shear layer. This further implies that the interaction between the flow/pressure fluctuations at two branches was particularly intense and resulted in the uncommon mode change.

To explain the mode change, a conceptual model is presented:

When the fluid flow starts to supply, the shear layer in the first branch induces the acoustic resonance at the third mode ( $m = 2$ ) at first, actually the shear flow has oscillate at the same mode ( $St = 0.4$ ) with that under  $Q = (5.5+31)$  l/min. Then this third mode fluctuation flows through the main pipe and goes into the second branch. When the flow rate is smaller than  $(5.5 + 29)$  l/min, the second branch acts just a resonator. However, when the flow rate over  $(5.5 + 30)$  l/min, the amplitude of oscillation in the second branch becomes high enough to propagate into the main pipe and impinges on the flow from the shear layer of the first branch at the impingement point, as shown in Fig. 6. This impingement inhibits the growth of the third acoustic mode in the first branch and makes the first acoustic mode becomes the dominant mode in the whole tandem system. In other word, it is the pressure fluctuation which feedback from the second branch to the first branch that inhibits the growth of the third acoustic mode in the first branch and makes the whole tandem system dominates at the first acoustic mode.

## 4 Conclusions

The high-time-resolved PIV technique can detect the time sequential instantaneous velocity field oscillating at a high frequency. The dominant frequency and the phase difference were obtained from the PIV data. Measured frequency was in good agreement with the results obtained from the empirical equation and the microphone.

The contour maps of phase differences in the first branch for  $Q = (5.5+28)$  l/min and  $Q = (5.5+31)$  l/min were obtained. The results can illustrate the relation between the shear flow and the edge, and it can be used to discuss the pressure feedback from the second branch or the whole system to the flow in the first branch effectively.

An uncommon mode change (from higher acoustic mode to lower mode) was observed. To explain this mode change, a conceptual model is presented, but more study should be done to prove the model.

## References

- 1) S. Ziada, E.T. Bühlmann: *Journal of Fluids and Structures*, 6, 583-601, (1992).
- 2) S. Ziada, S. Shine: *Journal of Fluids and Structures*, 13, 127-142, (1999).
- 3) W.M. Jungowski, K.K. Botros, W. Studzinski: *Journal of Sound and Vibration*, 131(2), 265-285, (1989).